Appl Microbiol Biotechnol (2014) 98:8155–8164
DOI 10.1007/s00253-014-5895-0

Metabolic engineering of *Saccharomyces cerevisiae* for itaconic acid production

John Blazeck · Jarrett Miller · Anny Pan · Jon Gengler · Clinton Holden · Mariam Jamoussi · Hal S. Alper

Received: 28 March 2014 / Revised: 8 June 2014 / Accepted: 11 June 2014 / Published online: 5 July 2014

Abstract Renewable alternatives for petroleum-derived chemicals are achievable through biosynthetic production. Here, we utilize *Saccharomyces cerevisiae* to enable the synthesis of itaconic acid, a molecule with diverse applications as a petrochemical replacement. We first optimize pathway expression within *S. cerevisiae* through the use of a hybrid promoter. Next, we utilize sequential, in silico computational genome-scanning to identify beneficial genetic perturbations that are metabolically distant from the itaconic acid synthesis pathway. In this manner, we successfully identify three non-obvious genetic targets (Δ*ade3* Δ*bna2* Δ*tes1*) that successively improve itaconic acid titer. We establish that focused manipulations of upstream pathway enzymes (localized refactoring) and enzyme relocalization to both mitochondria and cytosol fail to improve itaconic acid titers. Finally, we establish a higher cell density fermentation that ultimately achieves itaconic acid titer of 168 mg/L, a sevenfold improvement over initial conditions. This work represents an attempt to increase itaconic acid production in yeast and demonstrates the successful utilization of computationally guided genetic manipulation to increase metabolic capacity.

Keywords Itaconic acid · Metabolic engineering · *Saccharomyces cerevisiae* · Flux balance analysis · Genome-scale metabolic engineering

Electronic supplementary material The online version of this article (doi:10.1007/s00253-014-5895-0) contains supplementary material, which is available to authorized users.

J. Blazeck · J. Miller · A. Pan · C. Holden · M. Jamoussi · H. S. Alper (✉)
McKetta Department of Chemical Engineering, The University of Texas at Austin, 200 E Dean Keeton St. Stop C0400, Austin, TX 78712, USA
e-mail: halper@che.utexas.edu

J. Gengler
Department of Chemistry & Biochemistry, The University of Texas at Austin, 105 E 24th St. Stop A5300, Austin, TX 78712, USA

H. S. Alper
Institute for Cellular and Molecular Biology, The University of Texas at Austin, 2500 Speedway Avenue, Austin, TX 78712, USA

Introduction

Microbial conversion of renewable feedstock into commodity and specialty chemicals provides a unique alternative to a petroleum-based economy (Atsumi et al. 2008; Curran and Alper 2012; Keasling 2010; Schirmer et al. 2010). In this regard, itaconic acid is an attractive, naturally produced, versatile monomer that was named a top 12 value-added chemical from biomass by the Department of Energy in 2004 (Werpy and Petersen 2004). The theoretical yield of itaconic acid from glucose is 64.1 %, assuming the production of one molecule itaconic acid per one hexose molecule and the loss of a single carbon dioxide molecule during conversion (Bonnarme et al. 1995). Itaconic acid has diverse applications both as a copolymer for traditional petro-derived plastics and rubbers (Okabe et al. 2009; Tate 1981; Tsai et al. 2000) and as polymerized polyitaconic acid, a functional alternative to petroleum-derived polyacrylic acid (Nuss and Gardner 2013; Okabe et al. 2009). However, the expanding market for itaconic acid-derived products is dependent on a concurrent decrease in production costs (Nuss and Gardner 2013; Okabe et al. 2009) and a move towards a more tractable, easy-to-cultivate host system. To this end, here we describe the metabolic engineering of *Saccharomyces cerevisiae* for itaconic acid production.

Itaconic acid production was first observed in *Aspergillus itaconicus* in 1932 (Kinoshita 1932) and current industrial fermentation production utilizes a related strain, *Aspergillus*

terreus (Tevz et al. 2010). While rational engineering of *Aspergillus* species has improved itaconic acid titers to 1.4 g/L (Blumhoffa et al. 2013; Li et al. 2012), the high titers required for industrial production (of more than 80 g/L) have been enabled by efforts utilizing media optimization and large-scale mutagenesis (Kautola et al. 1991; Kuenz et al. 2012; Yahiro et al. 1995). Despite the high itaconic acid titers enabled in *A. terreus* fermentations, this organism has several drawbacks including being (1) naturally inhibited in media formulated to induce production and (2) negatively impacted by shear stress, preventing cultivation in standard stirred tank bioreactors (Park et al. 1994; Tevz et al. 2010; Yahiro et al. 1995). Metabolic profiling and functional gene characterization in *A. terreus* demonstrated that itaconic acid production proceeds through the decarboxylation of *cis*-aconitic acid, a tricarboxylic acid (TCA) cycle intermediate (Bonnarme et al. 1995) via the *cis*-aconitic acid decarboxylase encoding gene (CAD) (Kanamasa et al. 2008) (Fig. 1a). Thus, the potential to import the CAD gene into a model host organism opens the possibility to increase itaconic acid biosynthetic capacity while avoiding logistical difficulties inherent in *A. terreus* cultivations. To date, very limited or unpublished attempts have been undertaken to utilize non-*Aspergillus* microorganisms for itaconic acid production (Liao et al. 2010; Lin 2011).

Here, we report on an engineering effort in the model yeast, *S. cerevisiae*, for itaconic acid production. *S. cerevisiae* has a fully developed genetic toolbox to enable rational metabolic engineering approaches and has become a standard host for biosynthetic production and metabolic engineering (Nevoigt 2008). *S. cerevisiae* offers numerous advantages towards industrial fermentations including robust growth in low pH and lower temperatures, high tolerance to shear stress, lack of phage contamination, and ease of separation (Liu et al. 2013). Itaconic acid production was enabled by importing the *cis*-aconitic decarboxylase gene, and titers were further enhanced by engineering native metabolism. Specifically, in silico genome-scale stoichiometric models were used to quickly identify non-obvious genetic effectors that increase desired metabolic flux (Alper et al. 2005b; Blazeck and Alper 2010; Lee et al. 2012; Lerman et al. 2012). We utilized a sequential, computationally guided selection of three genetic targets to enhance production. Through this work, we combine three approaches: (1) overexpression of the CAD enzyme with a synthetic hybrid promoter, (2) the sequential deletion of the *ade3*, *bna2*, and *tes1* genes, and (3) high cell density fermentation. Collectively, these approaches improved itaconic acid titer sevenfold (to 168 mg/L) over a strain simply expressing the *CAD1* gene. This work represents an attempt to increase organic acid production in yeast and demonstrates the successful utilization of model-guided metabolic perturbations to increase product titer in a fungal host.

Materials and methods

Strains and media

Yeast expression vectors were propagated in *Escherichia coli* DH10B. *E. coli* DH10B was routinely cultivated in LB Media Broth (Teknova) supplemented with 50 μg/ml ampicillin for plasmid propagation at 37 °C with constant shaking. All yeast strains originated from *S. cerevisiae* BY4741 (MATa; his3Δ1; leu2Δ0; met15Δ0; ura3Δ0) obtained from EUROSCARF, Frankfurt, Germany. Yeast strains were routinely cultivated at 30 °C with constant agitation in yeast synthetic complete (YSC) media, containing 20 g/L glucose (Fisher Scientific), 0.67 g/L yeast nitrogen base (Becton, Dickinson, and Company), and a Complete Supplement Mixture (CSM) amino acid dropout supplement (MP Biomedicals). YSC-URA, YSC-URA-LEU, and YSC-URA-LEU-HIS contained 0.77 g/L CSM-Uracil, 0.67 g/L CSM-Uracil-Leucine, and 0.65 g/L CSM-Uracil-Leucine-Histidine, respectively. To induce expression of a Cre-Recombinase gene, yeast strains were cultivated in a media similar to YSC-URA called YSC-URA-gal that contained 20 g/L galactose (Fisher Scientific) instead of glucose. Yeast strains were cultivated in yeast extract peptone dextrose (YPD) prior to transformations. YPD media contained 40 g/L glucose, 40 g/L peptone (Fisher Scientific), and 20 g/L yeast extract (Fisher Scientific). Solid media for *E. coli* and *S. cerevisiae* were prepared by adding 20 g/L agar (Teknova) to liquid media. YSC media and YPD plates were supplemented with 200 μg/mL G418 as needed.

Cloning procedures

All restriction enzymes were purchased from New England Biolabs, and all digestions were performed according to standard protocols. PCR reactions were set up with recommended conditions using phusion high fidelity DNA polymerase (Finnzymes). Ligation reactions were performed overnight at room temperature using T4 DNA Ligase (Fermentas). Gel extractions were performed using the Fermentas GeneJET Extraction Kit (Fisher Scientific). *E. coli* minipreps were performed using the Zyppy Plasmid Miniprep Kit (Zymo Research Corporation). Transformation of *E. coli* strains was performed using the standard electroporator protocols (Sambrook and Russell 2001). Transformation of *S. cerevisiae* with plasmid DNA was performed using the Zymogen Frozen EZ Yeast Transformation Kit II (Zymo Research Corporation). Transformation of *S. cerevisiae* with linearized DNA was performed using the Hegemann Protocol (Guldener et al. 1996). Genomic DNA was extracted from *S. cerevisiae* using the Wizard Genomic DNA Purification Kit (Promega), and BY4741 genomic DNA (gDNA) was routinely utilized as template for PCR. Plasmids were isolated from *S. cerevisiae* using the Yeast Miniprep Kit I (Zymo Research Corporation).

Plasmid construction

All plasmids containing expression cassettes were sequence confirmed before transformation into *S. cerevisiae*. Table S1 contains all primer sequences, and a full description of plasmid construction can be found in the supplementary online material, but a more concise description follows. Plasmids p416-MCS-yECitrine, p416-MCS-Cyc, p416-MCS-Tef, p416-MCS-GPD, p416-UAS_{TEF}-UAS_{CIT}-UAS_{CLB}-Gpd, p415-GPD, p413-GDP, and p41K-GPD have been described (Blazeck et al. 2012; Karim et al. 2013; Mumberg et al. 1995). These plasmids were originally derived from the Mumberg plasmid set. They utilize a CEN-ARS for low copy replication but vary in selection marker as follows: p416 plasmids alleviate uracil auxotrophy, p415 plasmids alleviated leucine auxotrophy, p413 plasmids alleviate histidine auxotrophy, and p41K plasmids confer resistance to G418.

The *cis*-aconitic acid decarboxylase encoding cDNA (CAD) from *A. terreus* (DNA data bank of Japan accession number AB326105) (Kanamasa et al. 2008) was codon optimized after the removal of one intron for expression in *S. cerevisiae* (submitted to NCBI GenBank database under accession number KJ653453) and inserted into plasmids p416-MCS-Cyc, p416-MCS-Tef, p416-MCS-GPD, and p416-UAS_{TEF}-UAS_{CIT}-UAS_{CLB}-Gpd. The UAS_{TEF}-UAS_{CIT}-UAS_{CLB}-Gpd-CAD expression cassette was inserted into a p426 vector for multicopy overexpression.

Citrate synthases and pyruvate carboxylase genes, including CIT1 (NCBI GenBank accession number NM_001183178.1), CIT2 (GenBank accession number NM_001178718.1), PYC1 (GenBank accession number NM_001180927.1), and PYC2 (GenBank accession number NM_001178566.1) were inserted into a p415-GPD vector. PYC1 and PYC2 were also inserted into plasmid p413-GPD.

Four *S. cerevisiae* mitochondrial localization signals (MLS) (Table S2) were fused to the N′ terminus of the CAD gene (immediately after the start codon) in plasmid p416-UAS_{TEF}-UAS_{CIT}-UAS_{CLB}-Gpd-CAD using homologous recombination cloning. The COX4 MLS was also fused to the CAD gene in plasmids p416-Cyc-CAD and p416-Tef-CAD.

Aconitase (GenBank accession number NM_001182192.1) and citrate synthase enzymes (ACO1 and CIT1) were N′ terminally truncated to remove native MLS signals. ACO1 and ACO1 fragments truncated by 25, 37, and 50 amino acids were inserted into p415-GPD. Similarly, CIT1 and CIT1 fragments truncated by 25, 38, and 50 amino acids were inserted into p413-GPD. CIT-50 was also inserted into plasmid p41K-GPD.

Strain construction

All strains were confirmed through genomic DNA extraction and PCR confirmation. Single knockout BY4741 strains shown in Fig. 2 were isolated from the yeast knockout collection (Winzeler et al. 1999) and transformed with plasmid p416-UAS_{TEF}-UAS_{CIT}-UAS_{CLB}-Gpd-CAD. A markerless BY4741 Δ*ade3* strain was constructed by replacing the wild-type *ADE3* gene with a kanMX resistance gene amplified from plasmid pUG6 (EUROSCARF) using primers JB775/776 and extended using primers JB777/778. After confirmation, this BY4741 Δ*ade3* $kanMX^+$ strain was transformed with plasmid pSH47 (EUROSCARF) and cultivated in YSC-URA-gal to induce expression of Cre-Recombinase, then cultivated in YPD media to lose plasmid pSH47. Replica plating and genotypic confirmation enabled isolation of a BY4741 Δ*ade3* strain lacking the KanMX resistance marker and pSH47.

Double knockout strains shown in Fig. 3 were created by isolating gDNA from single knockout strains from the yeast knockout collection (Winzeler et al. 1999), amplifying KanMX-replaced loci, and transforming these knockout cassettes into the markerless BY4741 Δ*ade3* strain. Knockout cassettes for *MET22*, *YNK1*, *PXA1*, *BNA5*, *BNA2*, *PYC1*, and *IDP1* were amplified from appropriate gDNA using primers JB844/845, JB826/827, JB824/825, JB828/829, JB840/841, JB838/839, and JB836/837, respectively. Resultant strains were transformed with plasmid p416-UAS_{TEF}-UAS_{CIT}-UAS_{CLB}-Gpd-CAD and assayed for itaconic acid production.

A markerless BY4741 Δ*ade3* Δ*bna2* strain was constructed using the protocol described above, except the kanMX resistance amplicon to be transformed into BY4741 Δ*ade3* was created using primers JB897/898 and elongated with JB899/900. Triple knockout strains shown in Fig. 4 were created by isolating gDNA from single knockout strains from the yeast knockout collection (Winzeler et al. 1999), amplifying KanMX-replaced loci, and transforming these knockout cassettes into the markerless BY4741 Δ*ade3* Δ*bna2* strain. Knockout cassettes for *UTR4*, *ADI1*, *BNA3*, *MEU1*, *MDE1*, *MRI1*, *SPE2*, *PXA1*, *TES1*, *YDC1*, *SCS7*, *SUR1*, *MET22*, *SHM1*, *TPO5*, *SPE3*, *FUM1*, and *PYC1* were amplified from appropriate gDNA using primers JB944/945, JB946/947, JB948/949, JB950/951, JB952/953, JB954/955, JB956/957, JB824/825, JB958/959, JB960/961, JB962/963, JB964/965, JB830/831, JB844/845, JB966/967, JB968/969, JB971/972, JB973/974, and JB838/839, respectively. Resultant strains were transformed with plasmid p416-UAS_{TEF}-UAS_{CIT}-UAS_{CLB}-Gpd-CAD and assayed for itaconic acid production.

Itaconic acid quantification

S. cerevisiae strains were routinely cultivated as described above for 3 days in 250-mL flasks glass bottles in 15 mL of appropriate YSC media. For initial characterization of knockout libraries, *S. cerevisiae* strains were cultivated in 2 mL YSC media for 3 days, and a secondary 15-mL cultivation was performed for strains exhibiting beneficial phenotypes. After

growth, a 1.0-mL sample was pelleted down for 3 min at 10,000×*g*, and supernatant was filtered using a 0.2-μm syringe filter (Corning Incorporated). Filtered supernatant was analyzed with a HPLC Ultimate 3000 (Dionex) and a Zorbax SB-Aq column (Agilent Technologies). A 2.0-μL injection volume was used in a mobile phase composed of a 99.5:0.5 ratio of 25 mM potassium phosphate buffer (pH=2.0) to acetonitrile with a flow rate of 1.25 mL/min. The column temperature was maintained at 30 °C and UV–Vis absorption was measured at 210 nm. An itaconic acid standard (Sigma-Aldrich) was used to detect and quantify itaconic acid production.

Flux balance analysis-mediated computational gene deletion analysis

The consensus reconstruction of yeast metabolism with compartmentalization (Herrgard et al. 2008) was uploaded into MATLAB R2009b (Mathworks) and manipulated with the Cobra Toolbox (Schellenberger et al. 2011) on a standard Dell desktop computer. *Cis*-aconitic acid decarboxylation and itaconic acid export reactions were added to the reaction matrix. Yeast metabolism was perturbed in silico through the individual deletion of every enzymatic reaction in the reaction matrix using the simpleOptKnock function. Resultant matrices were computationally analyzed with flux balance analysis to predict itaconic acid production. Glucose input was set to the standard 10 mmol/gDW/h. Itaconic acid export flux was utilized as a gauge of predicted itaconic acid production. Maximizing biomass accumulation was utilized as the system's objective function. Analysis of single knockouts and comparison to the initial model (wild-type) are shown in Fig. 2a and Table S3.

The reaction encoded by the Ade3p enzyme was deleted from the yeast reaction matrix, and computation analysis of the effect of single gene deletions on itaconic acid production in the *ade3* in silico background was performed to yield the results shown in Fig. 3a. The reaction encoded by the Bna2p enzyme was deleted from the yeast reaction matrix, and computation analysis of the effect of single gene deletions on itaconic acid production in the ade3 bna2 in silico background was performed to yield the results shown in Fig. 4a and Table S3. Seven in silico genetic knockouts not shown in Fig. 4a, Δ*utr4*, Δ*adi1*, Δ*bna3*, Δ*meu1*, Δ*mde1*, Δ*mri1*, and Δ*spe2*, were predicted to generate theoretical yield, a several hundred fold improvement.

Prediction of intracellular localization

Probability of mitochondrial protein localization was predicted using the MITOPROP II v1.101 program (Claros and Vincens 1996). In all cases, the entire protein's amino acid sequence was inputted. Native subcellular localizations were taken from the *Saccharomyces* Genome Database (Cherry et al. 2012).

Increased cell density fermentations

Biological triplicates of *S. cerevisiae* wild-type, Δ*ade3* Δ*bna2*, and the Δ*ade3* Δ*bna2* Δ*tes1* strains that carried a plasmid containing the Enhanced GPD-CAD expression cassette were cultivated as described above for 3 days in 250-mL flasks glass bottles in 15 mL of appropriate YSC media. After 3 days of cultivation, cultures were harvested by centrifugation at 1,000×*g* for 2 min and resuspended in 1-mL fresh YSC media. Appropriate volumes of these 1-mL cultures were added to 250-mL flasks glass bottles containing 15 mL of fresh YSC media to attain an initial OD_{600}=6.0. Cultures were cultivated as described above for 3 days and then assayed for itaconic acid production.

Results

Enabling fungal production of itaconic acid

To enable biosynthesis of itaconic acid in yeast, the *cis*-aconitic acid decarboxylase gene from *A. terreus* (Kanamasa et al. 2008) was codon optimized and inserted into autonomous yeast expression vectors. CAD expression was driven by one of several well-characterized promoters: P_{CYC}, P_{TEF}, and P_{GDP} promoters or by an "Enhanced P_{GPD}" promoter (UAS_{TEF}-UAS_{CIT}-UAS_{CLB}-P_{GPD}), an engineered hybrid promoter augmented by the 5′ addition of three tandem upstream activating sequences (Blazeck et al. 2012). Previous characterization demonstrated that these promoters encompass a wide range of gene expression capacity such that P_{CYC} < P_{TEF} < P_{GPD} < Enhanced P_{GPD} (Blazeck et al. 2012). *S. cerevisiae* BY4741 strains harboring CAD expression cassettes were cultivated and assayed for itaconic acid production (Fig. 1b). In each case, heterologous expression of the CAD gene enabled itaconic acid production, and titers improved with increased CAD expression to 59 mg/L, before plateauing between P_{GPD} and Enhanced P_{GPD} expression levels (Fig. 1b). To confirm that CAD expression was not limiting beyond this point, the Enhanced P_{GPD}-CAD expression cassette was inserted into a multicopy expression vector, and itaconic acid levels surprisingly decreased by 66 % (Table 1). Thus, the control of itaconic acid production through CAD expression can be maximized utilizing the Enhanced P_{GPD} promoter. Furthermore, these experiments highlight the need for metabolic rewiring to further improve titers. A time course of itaconic acid production by the B4741 strain harboring the Enhanced P_{GPD} CAD expression cassette revealed that itaconic acid production is completed within the first 3 days of fermentation (Fig. 1c), allowing the duration of future fermentations to be limited to 3 days in length.

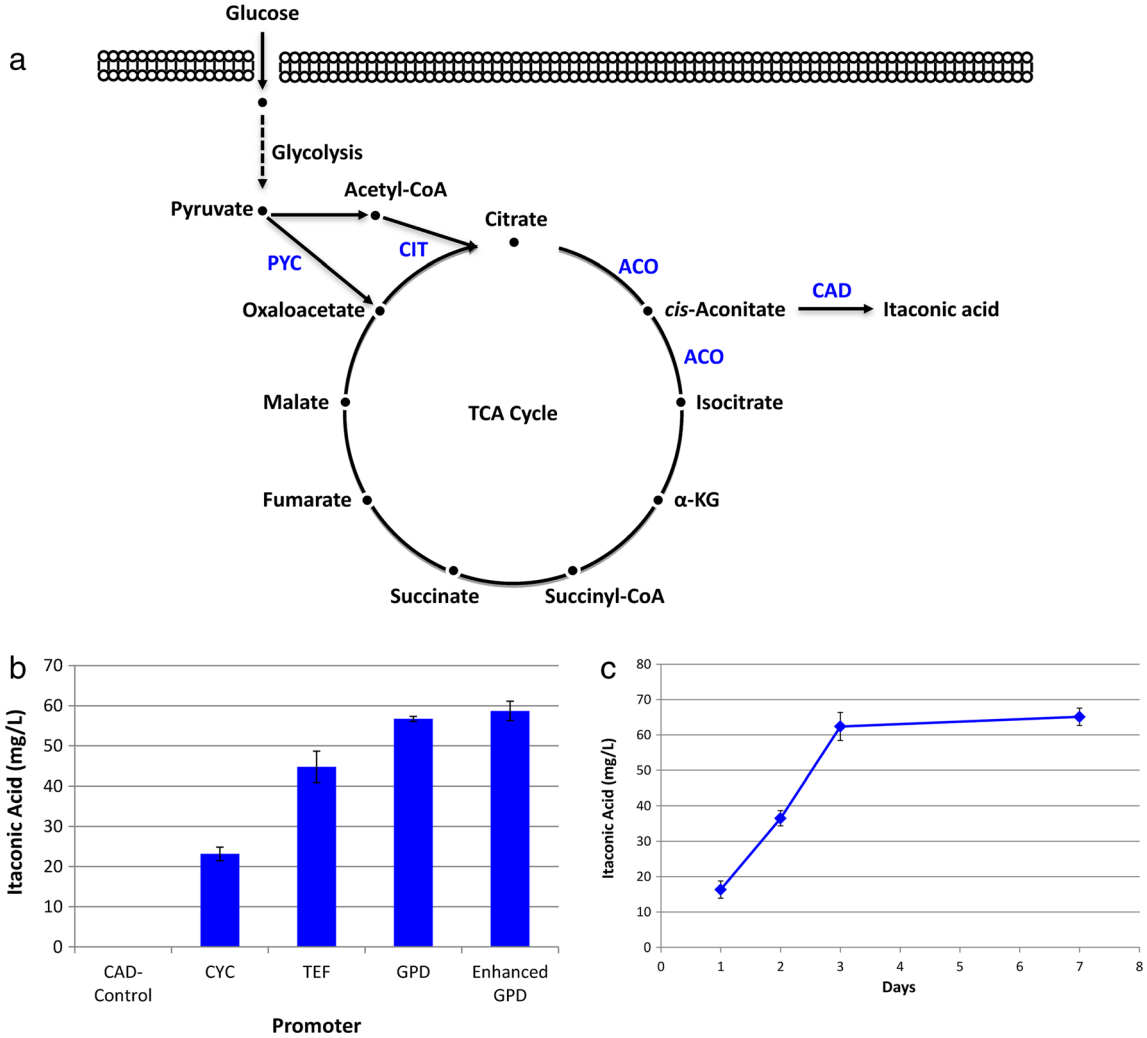

Fig. 1 Enabling itaconic acid production and optimizing CAD expression. **a** A simplified schematic is provided detailing the itaconic acid synthesis pathway from a citric acid cycle intermediate, *cis*-aconitic acid. Four enzymes directly involved in the itaconic acid synthesis pathway are shown in *blue*. *PYC* = pyruvate carboxylase, *CIT* = citrate synthase, *ACO* = aconitase, and *CAD* = *cis*-aconitic acid decarboxylase. **b** Importing CAD into BY4741 enables itaconic acid production. Increasing CAD expression increases itaconic acid titer and plateaus at roughly 59 mg/L when CAD expression is driven by the Enhanced P_{GPD} promoter. The CAD control represents the BY4741 strain lacking CAD expression and produces no itaconic acid, as expected. **c** A time course of itaconic acid production in a *S. cerevisiae* BY4741 strain harboring a CAD expression cassette driven by the Enhanced P_{GPD} promoter is shown. Itaconic acid production begins soon after the start of the fermentation and is finished by the third day. *Error bars* represent standard deviation from biological triplicates

Stoichiometric model-guided rewiring of *S. cerevisiae* metabolism to enhance itaconic acid titer

We utilized a genome-wide stoichiometric model to search for gene deletion targets that would improve total itaconic acid titer. To do so, we added the *cis*-aconitic acid decarboxylation and itaconic acid export reactions into the consensus genome-scale stoichiometric model of yeast metabolism (Herrgard et al. 2008) using the Cobra Toolbox (Schellenberger et al. 2011). Steady-state metabolic fluxes within the reaction network were calculated, and single genome deletion scans (Alper et al. 2005a) were conducted to identify genetic knockouts that could improve itaconic acid production. A total of 11 single gene knockouts were predicted to increase flux through the itaconic acid synthesis pathway (Fig. 2a and Table S3). Overall, these genetic targets were "non-obvious" in that they are not members of the local itaconic acid synthesis pathway. To compare in silico and in vivo itaconic acid production by these targets, we conducted small-scale cultivations (in test tubes) for the 11 computationally selected single gene deletion backgrounds (transformed with Enhanced P_{GPD}-CAD expression cassettes) and compared to production levels to that of the wild-type strain (Fig. 2b). Across the board, our analysis revealed large discrepancies between in silico and in vivo itaconic acid production phenotypes. However, four genetic deletions, Δ*ynk1*, Δ*fat1*, Δ*shm2*, and Δ*ade3*, improved in vivo titer (Fig. 2b). Thus, while the in silico gene identification was prone to many false positives, several advantageous targets

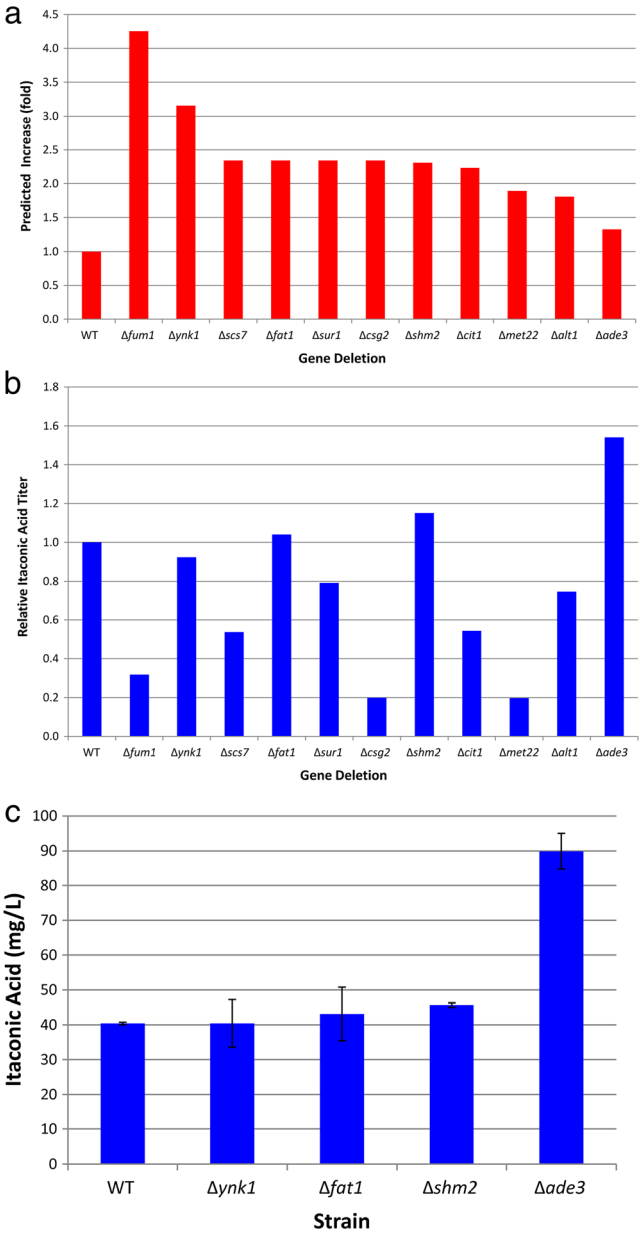

Fig. 2 Single gene deletion genome scan and in vivo testing to identify genetic effectors of itaconic acid synthesis. **a** In silico genome-scanning identified 11 gene deletions predicted to increase flux through the itaconic acid reaction. Results are shown as the relative yield increase compared to wild-type. **b** Small-scale cultivation revealed that in silico prediction did not correlate strongly with in vivo phenotype. Relative itaconic acid titers represent the ratio of the averages of biological duplicates. Standard deviations of biological duplicates were typically less than 20 %. Four deletion targets improved titers substantially enough to warrant **c** flask-scale confirmation of itaconic acid production. Of these four targets, Δ*ade3* deletion significantly increased itaconic acid titer to 90 mg/L. *WT* represents unmodified BY4741 production of itaconic acid. *Error bars* represent standard deviation from biological triplicates

were identified. Further analysis of the Δ*ynk1*, Δ*fat1*, Δ*shm2*, and Δ*ade3* deletion strains in flask-scale cultivations highlighted one knockout, Δ*ade3*, as the lead candidate that significantly improved itaconic acid titer to 90 mg/L (Fig. 2c).

Thus, we sought to invoke an iterative search for gene deletions via a greedy algorithm to further increase itaconic acid titer, using the Δ*ade3* deletion strain as our starting point.

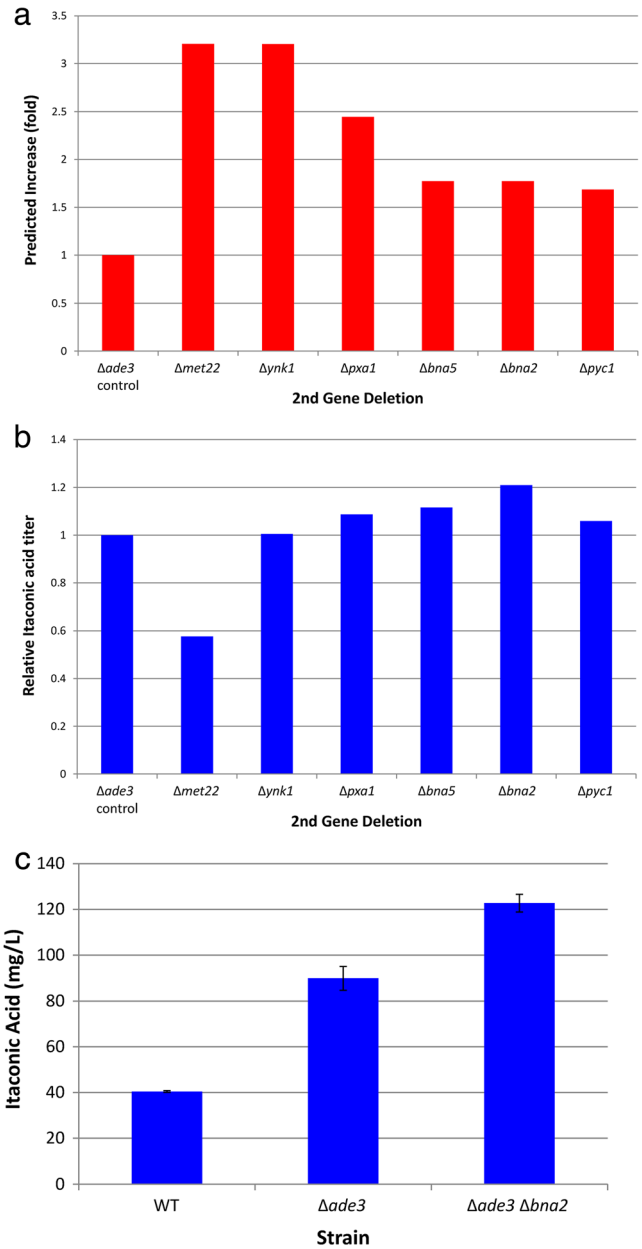

Fig. 3 Selecting secondary deletion targets for enhanced itaconic acid synthesis. **a** In silico genome-scanning of a Δ*ade3* reaction matrix identified six gene deletions predicted to increase itaconic acid yield in the Δ*ade3* background. Results are shown as the relative yield increase compared to predict for the *ade3* model. **b** Small-scale cultivation again revealed that in silico prediction did not correlate strongly with in vivo phenotype. Relative itaconic acid titers represent the ratio of the averages of biological triplicates. Standard deviations of biological triplicates were typically less than 20 %. **c** Flask-scale confirmation of itaconic acid production in the Δ*ade3* Δ*bna2* background increased titer to 122 mg/L. *WT* represents unmodified BY4741 production of itaconic acid. *Error bars* represent standard deviation from biological triplicates

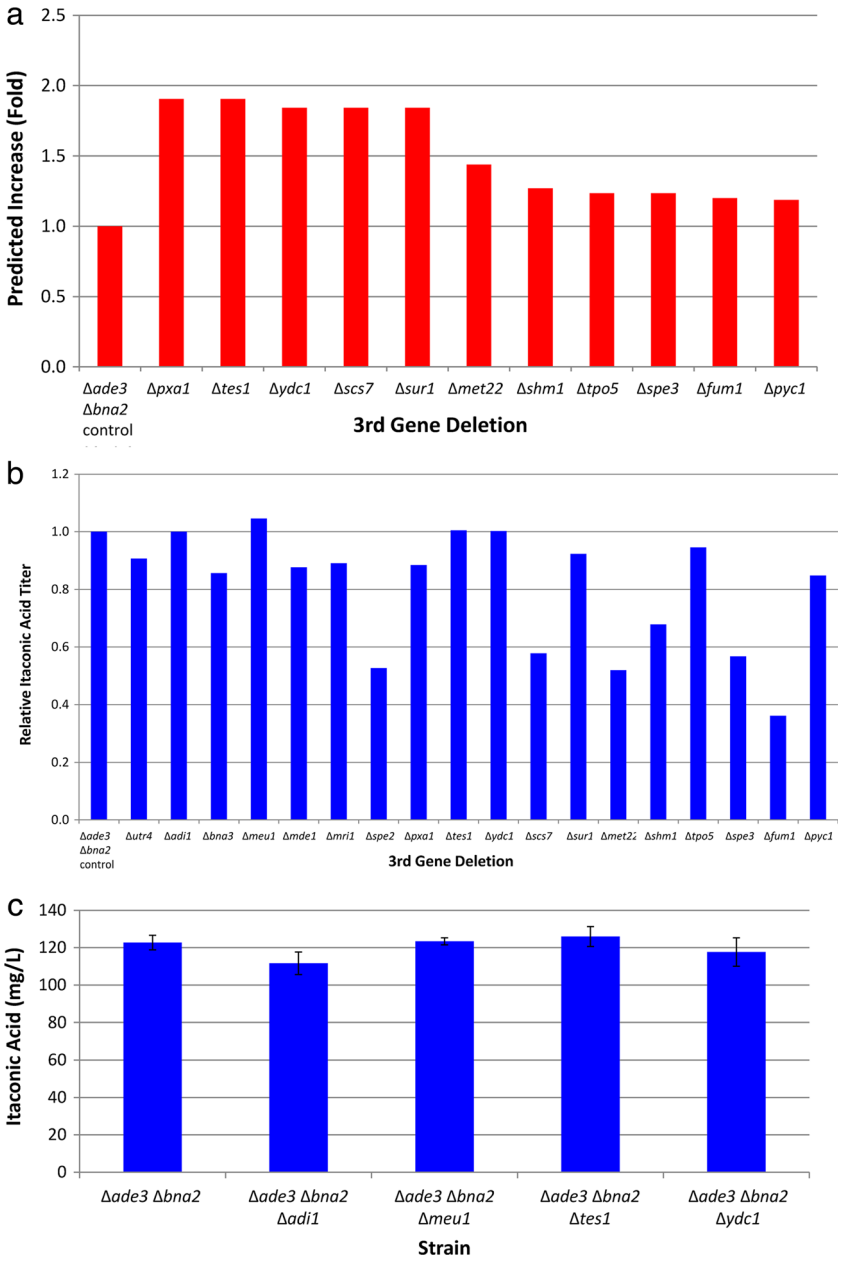

Fig. 4 Selecting tertiary deletion targets for enhanced itaconic acid synthesis. **a** In silico genome-scanning of a Δ*ade3* Δ*bna2* reaction matrix identified 18 gene deletions predicted to increase itaconic acid yield in the Δ*ade3* Δ*bna2* background. Results are shown for 11 of these targets as a relative increase compared to predicted flux for the Δ*ade3* Δ*bna2* model, as the other seven targets were predicted to generate theoretical yield (a ~10^6-fold increase in flux). **b** Small-scale cultivation again revealed that in silico prediction did not correlate strongly with in vivo phenotype. Relative itaconic acid titers represent the ratio of the averages of biological triplicates. Standard deviations of biological triplicates were typically less than 10 %. **c** Flask-scale cultivation of the Δ*ade3* Δ*bna2* Δ*tes1* background enabled increased itaconic acid titer to 126 mg/L. *Error bars* represent standard deviation from biological triplicates

The Ade3p enzymatic reaction was deleted from the metabolic reconstruction containing the itaconic acid pathway (in silico), and a markerless Δ*ade3* null strain was constructed (in vivo). Six gene targets were identified in silico as potential itaconic acid enhancers through a second genome scan (Fig. 3a and Table S3). While several of these targets demonstrated slight increases in itaconic acid during small-scale cultivations (Fig. 3b), only the Δ*bna2* deletion in an Δ*ade3* null background enabled an increase in itaconic acid titer during flask-scale cultivation, achieving upwards of 122 mg/L (Fig. 3c). Altered metabolic backgrounds often require re-optimization of pathway expression levels. Thus, we re-analyzed itaconic acid production in the Δ*ade3* Δ*bna3* background utilizing the multicopy Enhanced P_{GPD}-CAD expression vector. Once again, itaconic acid production was drastically reduced (Table 1), re-establishing that the point of optimal CAD expression was achieved using a lower copy vector with Enhanced P_{GPD} promoter.

Table 1 Ratio of itaconic acid production enabled by multicopy plasmid CAD expression to singly copy CAD expression

Strain	Relative production (compared to single copy)
WT	0.34
Δ*ade3* Δ*bna2*	0.49

Despite the diminished returns between the first and second round target (Δ*ade3* increased titers around 100 %, whereas Δ*bna2* only increased titers around 20 %), we reiterated the sequential search for gene deletions to identify any putative third gene deletion targets. To accomplish this, the Bna2p enzymatic reaction was deleted from the ΔADE3p metabolic reconstruction and a markerless Δ*ade3* Δ*bna2* null strain was constructed. Seventeen targets were predicted to improve itaconic acid production in silico (Fig. 4a and Table S3), with seven knockouts not shown (Δ*utr4*, Δ*adi1*, Δ*bna3*, Δ*meu1*, Δ*mde1*, Δ*mri1*, and Δ*spe2*) predicted to generate the theoretical yield. In vivo confirmation with small-scale cultivations revealed no significant improvements for any of these triple knockout constructs (Fig. 4b), although the Δ*tes1* deletion in the Δ*ade3* Δ*bna2* deletion background produced an itaconic acid titer of 126 mg/L during flask-scale cultivations (Fig. 4c). Thus, in silico stoichiometric modeling successfully identified three genetic modifications (residing in distant, distinct metabolic pathways) that rewired metabolic flux to increase in vivo itaconic acid production.

Localized refactoring and retargeting of TCA cycle enzymes fail to enhance itaconic acid titer

Since itaconic acid biosynthesis stems from a tightly regulated TCA cycle intermediate (Fig. 1a), we attempted to increase titers by a partial refactoring of TCA cycle flux to increase *cis*-aconitic acid availability. Specifically, we upregulated the CIT1 (YNR001C) or CIT2 (YCR005C) citrate synthase and the PYC1 (YGL062W) or PYC2 (YBR218C) pyruvate carboxylase enzymes through constitutive P_{GPD} overexpression. However, neither single enzyme overexpressions nor co-overexpression of CIT1/PYC1, CIT1/PYC2, and CIT2/PYC1 enzyme pairs improved itaconic acid titer (Fig. 5a). Similarly, overexpression of the ACO1 (YLR304C) aconitase enzyme and co-overexpression of CIT1/ACO1 failed to increase titer in wild-type backgrounds (Fig. 5b). As a further attempt to rewire the structure of this biosynthetic pathway, we attempted enzyme re-localization. CAD-mediated synthesis of itaconic acid is cytosolic, but precursor synthesis is localized in the mitochondria. Mitochondrial or cytosolic localization of enzymatic pathways that utilize TCA metabolites has proven equally beneficial towards increasing pathway flux (Avalos et al. 2013; Brat et al. 2012). However, localization of the complete itaconic acid synthesis pathway, by either (1) targeting the CAD enzyme to mitochondria (Table S2 and Figs. S1 and S2) or (2) co-localizing the citrate synthase (CIT1) and aconitase (ACO1) mitochondrial-targeted enzymes to the cytoplasm (Fig. S3 and S4), did not improve itaconic acid production. Mitochondrial protein localization was predicted computationally, without in vivo confirmation.

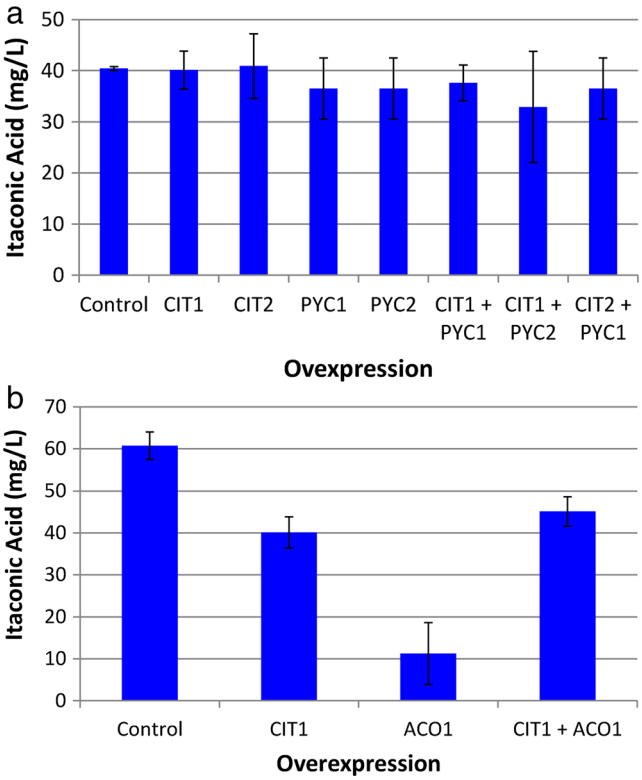

Fig. 5 TCA enzymatic overexpression fails to improve itaconic acid titer. **a** Citrate synthase (CIT1 or CIT2) and pyruvate carboxylase (PYC1 or PYC2) enzymes (Fig. 1a) were co-overexpressed with the CAD enzyme but failed to increase itaconic acid titer compared to control (only CAD expression). **b** Similarly, citrate synthase (CIT1) and aconitase (ACO1) enzymes (Fig. 1a) failed to increase itaconic acid titer. *Error bars* represent standard deviation from biological triplicates

Enhancing itaconic acid titer with increased density fermentations

Finally, we sought to improve itaconic acid titer through higher cell density cultivations (initial OD_{600}=6.0). Fermentations were conducted for three strains: wild-type, Δ*ade3* Δ*bna2*, and the Δ*ade3* Δ*bna2* Δ*tes1* strain. Each of these strains carried a plasmid containing the CAD gene driven by the Enhanced GPD promoter. The higher cell density fermentations resulted in increased itaconic acid titer for each background (Fig. 6). This increase is attributable to a reduction in nutrient load necessary for biomass production. In particular, the Δ*ade3* Δ*bna2* Δ*tes1* background produced 168 mg/L itaconic acid (Fig. 6), a more than sevenfold improvement over our initial strain and conditions (wild-type background utilizing low-strength CAD expression from the P_{CYC} promoter). Moreover, the improvement seen in this triple knockout strains was most pronounced in this higher cell density fermentation which indicates that future work with controlled, large-scale bioreactor fermentations could further improve itaconic acid titer.

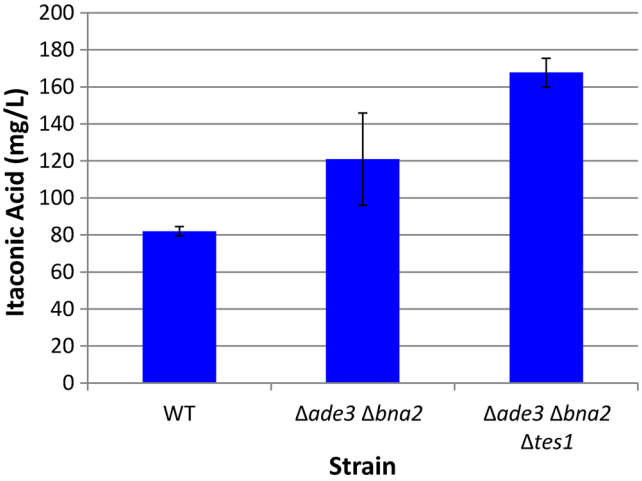

Fig. 6 Higher cell density fermentation improves itaconic acid production. **a** Fermentations beginning at an initial OD_{600}=6.0 increased itaconic acid titer for wild-type, Δ*ade3* Δ*bna2*, and Δ*ade3* Δ*bna2* Δ*tes1* strains (containing the Enhanced-P_{GDP}-CAD expression cassette). The Δ*ade3* Δ*bna2* Δ*tes1* background produced 168 mg/L itaconic acid, a more than sevenfold improvement over our initial strain and conditions. *Error bars* represent standard deviation from biological triplicates

Discussion

Here, we enable the synthesis of itaconic acid in *S. cerevisiae* and utilize a computationally guided selection of three genetic knockout targets to enhance production. We further establish that perturbations of TCA cycle enzymes that operate directly within the context of itaconic acid synthesis (by controlling *cis*-aconitic acid availability) have no effect on downstream flux and production. Similarly, mitochondrial or cytosolic localization of enzymes necessary for itaconic acid synthesis does not improve titer. Instead, genome-scale in silico modeling was able to successfully identify non-rational targets that function outside of the itaconic acid synthesis pathway. For instance, Ade3p (encoded by YGR204W) is a cytoplasmic trifunctional C1-tetrahydrofolate (THF) synthase involved in purine biosynthesis whose deletion produces histidine and adenine auxotrophies in yeast (Song and Rabinowitz 1993). We hypothesize that reducing metabolic flux towards amino acid synthesis through removal of Ade3p affords the observed increase in itaconic acid production. The Δ*ade3* deletion doubled itaconic acid titer in our system (Fig. 2c), far more than the ~30 % increase predicted in silico (Fig. 2a). This discrepancy further illustrates the inaccuracy yet utility of flux-based predictive analyses in yeast for identifying "non-obvious" targets. Similar to the Δ*ade3* mutant, removal of Bna2p catalytic activity could reduce metabolic flux towards amino acid synthesis, thereby increasing itaconic acid production. Bna2p (encoded by YJR078W) is a putative tryptophan 2,3-dioxygenase or indoleamine 2,3-dioxygenase, necessary for de novo biosynthetic NAD production from tryptophan (Panozzo et al. 2002). The non-statistically significant improvement generated via deletion of the Tes1p (encoded by YJR019C) peroxisomal acyl-CoA thioesterase (Jones et al. 1999) demonstrates that our systems-guided optimization of yeast metabolism likely attained an in silico local or global maximum in the itaconic acid production phenotypic landscape, limiting its effectiveness towards further advantageous gene knockout target identification. However, the sequential Δ*ade3*, Δ*bna2*, and Δ*tes1* deletions resulted in successful improvement of itaconic acid titer to 168 mg/L, a sevenfold improvement over initial conditions.

As a single copy of the CAD enzyme has been shown to enable production of high titers of itaconic acid in *Aspergillus* species (Kuenz et al. 2012) and multicopy CAD overexpression did not improve titer in a wild-type or Δ*ade3* Δ*bna2* background, it is unlikely that CAD enzyme activity is limiting production. Instead, we hypothesize that limited availability of the aconitic acid substrate prevents higher itaconic acid titer. In this regard, each iterative genetic deletion of Ade3p, Bnas2p, and Tes1p likely rewired intracellular metabolism to increase flux towards the citric acid cycle as we approached our final engineered strain. While the final titers achieved do not approach those in *Aspergillus* species, this strain can serve as a basis for further engineering of itaconic acid production in *S. cerevisiae*. Specifically, carbon flux has to be further accumulated within the citric acid cycle, potentially by importing exogenous TCA cycle enzymes from *Aspergillus* species or other described citric acid producers.

Acknowledgments This work was funded by the DuPont Young Professor Grant. We would like to thank Dr. Gary T. Rochelle for access to a HPLC and Alex Voice, Paul Nielsen, Nathan Fine, and Omkar Namjoshi for HPLC assistance.

References

Alper H, Jin YS, Moxley JF, Stephanopoulos G (2005a) Identifying gene targets for the metabolic engineering of lycopene biosynthesis in *Escherichia coli*. Met Eng 7(3):155–164

Alper H, Miyaoku K, Stephanopoulos G (2005b) Construction of lycopene-overproducing *E. coli* strains by combining systematic and combinatorial gene knockout targets. Nat Biotechnol 23(5): 612–616

Atsumi S, Hanai T, Liao JC (2008) Non-fermentative pathways for synthesis of branched-chain 8 higher alcohols as biofuels. Nature 451(7174):86–89

Avalos JL, Fink GR, Stephanopoulos G (2013) Compartmentalization of metabolic pathways in 10 yeast mitochondria improves the production of branched-chain alcohols. Nat Biotechnol 31(4):335–341

Blazeck J, Alper H (2010) Systems metabolic engineering: genome-scale models and beyond. Biotechnol J 5(7):647–659

Blazeck J, Garg R, Reed B, Alper H (2012) Controlling promoter strength and regulation in *Saccharomyces cerevisiae* using synthetic hybrid promoters. Biotechnol Bioeng 109(11):2884–2995

Blumhoffa ML, Steigera MG, Mattanovicha D, Sauera M (2013) Targeting enzymes to the right compartment: metabolic engineering for itaconic acid production by *Aspergillus niger*. Met Eng 19:26–32

Bonnarme P, Gillet B, Sepulchre AM, Role C, Beloeil JC, Ducrocq C (1995) Itaconate biosynthesis in *Aspergillus terreus*. J Bacteriol 177(12):3573–3578

Brat D, Weber C, Lorenzen W, Bode HB, Boles E (2012) Cytosolic relocalization and optimization of valine synthesis and catabolism enables increased isobutanol production with the yeast *Saccharomyces cerevisiae*. Biotechnol Biofuels 5:65

Cherry JM, Hong EL, Amundsen C, Balakrishnan R, Binkley G, Chan ET, Christie KR, Costanzo MC, Dwight SS, Engel SR et al (2012) *Saccharomyces* Genome Database: the genomics resource of budding yeast. Nucl Acid Res 40(D1):D700–D705

Claros MG, Vincens P (1996) Computational method to predict mitochondrially imported proteins and their targeting sequences. Eur J Biochem 241(3):779–786

Curran K, Alper H (2012) Expanding the chemical palate of cells by combining systems biology and metabolic engineering. Met Eng 14(4):289–297

Guldener U, Heck S, Fiedler T, Beinhauer J, Hegemann JH (1996) A new efficient gene disruption cassette for repeated use in budding yeast. Nucl Acid Res 24(13):2519–2524

Herrgard MJ, Swainston N, Dobson P, Dunn WB, Arga KY, Arvas M, Bluthgen N, Borger S, Costenoble R, Heinemann M et al (2008) A consensus yeast metabolic network reconstruction obtained from a community approach to systems biology. Nat Biotechnol 26(10): 1155–1160

Jones JM, Nau K, Geraghty MT, Erdmann R, Gould SJ (1999) Identification of peroxisomal acyl-CoA thioesterases in yeast and humans. J Bio Chem 274(14):9216–9223

Kanamasa S, Dwiarti L, Okabe M, Park EY (2008) Cloning and functional characterization of the cis-aconitic acid decarboxylase (CAD) gene from *Aspergillus terreus*. Appl Microbiol Biotechnol 80(2): 223–229

Karim AS, Curran KA, Alper HS (2013) Characterization of plasmid burden and copy number in *Saccharomyces cerevisiae* for optimization of metabolic engineering applications. Fems Yeast Res 13(1): 107–116

Kautola H, Rymowicz W, Linko YY, Linko P (1991) Itaconic acid production by immobilized *Aspergillus terreus* with varied metal additions. Appl Microbiol and Biotechnol 35(2):154–158

Keasling JD (2010) Manufacturing molecules through metabolic engineering. Science 330(6009):1355–1358

Kinoshita K (1932) Über die Production von Itaconsäure und Mannit durch einem neuen Schimmelpilz *Aspergillus itaconicus*. Acta Phytochim 5:271–287

Kuenz A, Gallenmuller Y, Willke T, Vorlop KD (2012) Microbial production of itaconic acid: developing a stable platform for high product concentrations. Appl Microbiol Biotechnol 96(5):1209–1216

Lee JW, Na D, Park JM, Lee J, Choi S, Lee SY (2012) Systems metabolic engineering of microorganisms for natural and non-natural chemicals. Nat Chem Biol 8(6):536–546

Lerman JA, Hyduke DR, Latif H, Portnoy VA, Lewis NE, Orth JD, Schrimpe-Rutledge AC, Smith RD, Adkins JN, Zengler K et al (2012) In silico method for modelling metabolism and gene product expression at genome scale. Nat Comm 3:929

Li A, Pfelzer N, Zuijderwijk R, Punt P (2012) Enhanced itaconic acid production in *Aspergillus niger* using genetic modification and medium optimization. Bmc Biotechnol 12:57

Liao JC, Chang PC; Industrial Technology Research Institute, assignee (2010) Genetically modified microorganisms for producing itaconic acid with high yields. USA

Lin T (2011) Engineering the production of itaconic acid in *Escherichia coli*. Houston, TX: Rice University. 76 p

Liu L, Redden H, Alper H (2013) Frontiers of yeast metabolic engineering: diversifying beyond ethanol and *Saccharomyces*. Curr Opinion Biotechnol 24:1023–1030

Mumberg D, Muller R, Funk M (1995) Yeast vectors for the controlled expression of heterologous proteins in different genetic backgrounds. Gene 156(1):119–122

Nevoigt E (2008) Progress in metabolic engineering of *Saccharomyces cerevisiae*. Microbiol Mol Biol Rev 72(3):379–412

Nuss P, Gardner KH (2013) Attributional life cycle assessment (ALCA) of polyitaconic acid production from northeast US softwood biomass. Int J Life Cycle Assess 18(3):603–612

Okabe M, Lies D, Kanamasa S, Park EY (2009) Biotechnological production of itaconic acid and its biosynthesis in *Aspergillus terreus*. Appl Microbiol Biotechnol 84(4):597–606

Panozzo C, Nawara M, Suski C, Kucharczyka R, Skoneczny M, Bécam AM, Rytka J, Herbert CJ (2002) Aerobic and anaerobic NAD+ metabolism in *Saccharomyces cerevisiae*. Febs Lett 517(1–3):97–102

Park YS, Itida M, Ohta N, Okabe M (1994) Itaconic acid production using an air-lift bioreactor in repeated batch culture of *Aspergillus terreus*. J Ferment Bioeng 77(3):329–331

Sambrook J, Russell DW (2001) Molecular cloning: a laboratory manual. Cold Spring Harbor Laboratory Press, Cold Spring Harbor

Schellenberger J, Que R, Fleming RMT, Thiele I, Orth JD, Feist AM, Zielinski DC, Bordbar A, Lewis NE, Rahmanian S et al (2011) Quantitative prediction of cellular metabolism with constraint-based models: the COBRA Toolbox v2.0. Nat Prot 6(9):1290–1307

Schirmer A, Rude MA, Li XZ, Popova E, del Cardayre SB (2010) Microbial biosynthesis of alkanes. Science 329(5991):559–562

Song JM, Rabinowitz JC (1993) Function of yeast cytoplasmic C1-tetrahydrofolate synthase. Proc Natl Acad Sci U S A 90(7):2636–2640

Tate BE (1981) Itaconic acid and derivatives. In: Grayson M, Eckroth E, editors. Kirk-Othmer Encyclopedia of Chemical Technology. 3 ed. p 865–873

Tevz G, Bencina M, Legisa M (2010) Enhancing itaconic acid production by *Aspergillus terreus*. Appl Microbiol Biotechnol 87(5):1657–1664

Tsai YC, Huang MC, Lin SF, Su YC; National Science Council, assignee (2000) Method for the production of itaconic acid using *Aspergillus terreus* solid state fermentation. United States

Werpy T, Petersen G (2004) Top value added chemicals from biomass: volume I—results of screening for potential candidates from sugars and synthesis gas. U.S. Department of Energy

Winzeler EA, Shoemaker DD, Astromoff A, Liang H, Anderson K, Andre B, Bangham R, Benito R, Boeke JD, Bussey H et al (1999) Functional characterization of the *S. cerevisiae* genome by gene deletion and parallel analysis. Science 285(5429):901–906

Yahiro K, Takahama T, Park YS, Okabe M (1995) Breeding of *Aspergillus terreus* mutant TN-484 for itaconic acid production with high yield. J Ferment Bioeng 79(5):506–508